AD-A152 066 AN ELECTRO-OPTIC SPATIAL LIGHT MODULATOR FOR THERMOELASTIC GENERATION OF..(U) SPECTRON DEVELOPMENT LABS INC COSTA MESA CA DEC 84 SDL-85-2361-02 1/1

UNCLASSIFIED N00014-84-C-0058 F/G 20/1 NL

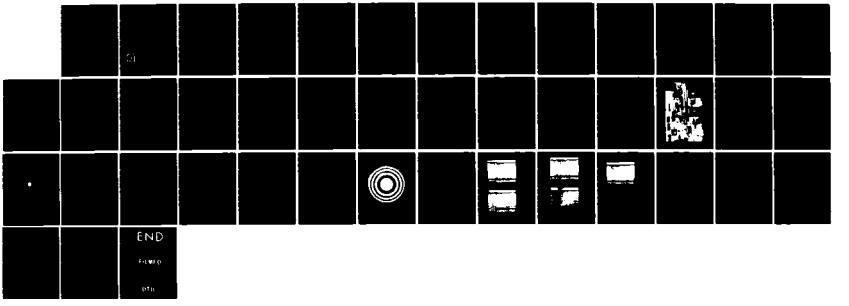

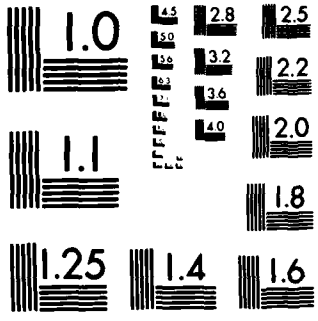

MICROCOPY RESOLUTION TEST CHART
NATIONAL BUREAU OF STANDARDS-1963 A

AN ELECTRO-OPTIC SPATIAL LIGHT MODULATOR FOR THERMOELASTIC GENERATION OF PROGRAMMABLY FOCUSED ULTRASOUND

FINAL REPORT

SDL No. 85-2361-02

December 1984

Prepared for:

Scientific Officer
Director
DEFENSE ADVANCED RESEARCH PROJECTS AGENCY
1400 Wilson Boulevard
Arlington, Virginia 22209
Attn: Dr. John Mesori

Under Contract No.
N00014-84-C-0058

The views and conclusions contained in this document are those of the authors and should not be interpreted as necessarily representing the official policies, either expressed or implied, of the Defense Advanced Research Projects Agency or the U.S. Government.

SDL
SPECTRON DEVELOPMENT LABORATORIES, INC.
3303 HARBOR BLVD., SUITE G-3, COSTA MESA, CA 92626 • (714) 549-8477

TABLE OF CONTENTS

LIST OF FIGURES

LIST OF TABLES

ABSTRACT

The concept proposed is an electro-optic technique that would make it possible to spatially modulate a high power pulsed laser beam to thermoelastically induce focused ultrasound in a test material. Being a purely electro-optic device, the modulator, and therefore the depth at which the acoustic focus occurs, can be programmed electronically at electronic speeds. If successful, it would become possible to scan ultrasound continuously in three dimensions within the component or structure under test.

1.0 IDENTIFICATION AND SIGNIFICANCE OF THE PROBLEM

The research presented here is an investigation of the feasibility of an electro-optic spatial light modulator that would make it possible to program at high speed the position and depth of focused ultrasound within a material under test. Ultrasonic nondestructive inspection (NDI) of materials and structures is becoming more pervasive in all business sectors, including defense, petroleum, construction and transportation. This is a consequence of increasing public concern about product safety and liability and the increasing commercial use of intrinsically hazardous processes and chemicals. Another important reason for increased NDI is economic. If a part can be proven to be sound, it need not be removed from service, as is currently done for some aircraft parts after a specified number of hours.

Ultrasonic inspection is performed by introducing, via a transducer, a directional beam of sound into the material under test. Most often the beam is physically scanned in a pattern designed to cover the area of interest, and one of two test modes is employed:

1. The Transmission Mode. The sound is introduced into one side of the material and measured on the other. If a flaw is intercepted by the beam, the amplitude of the received signal will be lower than that for an unflawed region. This method is commonly used for sheet materials, such as aircraft skin.

2. The Pulse Echo Mode. The sound is introduced into the material in the form of short pulses, and echos reflected from flaws are received. The distance to the flaw can be inferred by the transit time of the echo. The accuracy of both modes of operation is improved by reducing the cross-section of the ultrasonic beam, so that smaller flaws can be detected and large flaws accurately sized.

The dominant method used to generate the ultrasound is the piezo-electric transducer. These devices can be fabricated in many shapes and sizes and are quite efficient as both generators and receivers. Consequently, they often perform double duty in the pulse echo mode. The major disadvantage of this device is the need for coupling between the transducer face and the material, though this is not a devastating disadvantage in many cases, because testing can often be done in an immersion tank, or water jets or small fluid filled coupling bags can be used[1]. But the scan is still limited to mechanical velocities.

There are important instances, however, when physical coupling is not possible. This occurs when the material is too hot, too radioactive, or simply has a geometry too complex for the transducer and coupling device to follow. Recently, the Electro-Magnetic Acoustic Transducer (EMAT) was developed to overcome some of these objections[2]. The EMAT relies on the electro-magnetic generation of alternating eddy currents in the material, which in turn induce particle motion, and hence, elastic waves. Unfortunately, such transducers can operate only in ferro-magnetic materials, and their use is precluded in nonmetallic structures.

In the early 1960's White[3,4] proposed and demonstrated a partial solution to the difficulty of scanned ultrasound: thermoelastic generation of ultrasonic waves. By using a laser to thermally induce elastic stresses in the surface of the material, ultrasonic waves can be produced and scanned with the ease and speed of available optical techniques. Additionally, little or no surface preparation is required. However, if the surface characteristics are not optimum, incomplete absorption of the optical energy necessitates higher optical power levels to yield a given acoustic intensity. And the situation is further aggravated by the fact that the thermoelastic process is inherently inefficient, producing acoustic intensities four to seven orders of magnitude lower than the incident optical power. Hence, the optical intensities required to produce high acoustic energies within the sample approach and often surpass those levels that cause ablative damage to the surface of the material. But low optical power densities do produce sound, albeit at very low levels, and this has led to the idea that if the power density of the laser is distributed on the surface in proper temporal and/or spatial sequence, the low level generated sound can be made to focus at a desired location within the material. Thus, although the sound is generated over a broad region with a low optical power density, it will focus to a high acoustic intensity at the desired spot within the material.

The acoustic equivalent of the optical Fresnel zone plate[5] has been considered as the means by which this focusing of the ultrasonic energy might be accomplished. Unfortunately, a conventional Fresnel zone plate produces properly focused energy only at a predetermined

depth within the material. If one wishes to change this depth, or to actually scan it, that is possible only in discrete steps at mechanical speeds, unless a novel electronic programming of the zone plate can be devised. A promising approach to this problem is an electro-optic modulation technique in which the depth at which the energy is focused can be determined by electronic programing. It would offer speed and versatility, and would result in the capability of producing focused ultrasound that can be continuously scanned in three dimensions at electronic speeds.

2.0 BACKGROUND, TECHNICAL APPROACH, AND ANTICIPATED BENEFITS

2.1 Background and Technical Approach

The Phase I effort has been devoted to an investigation of the feasibility of a novel approach to electro-optic spatial light modulation. To understand the concept, consider the geometry of Figure 1, which illustrates the reverse of the acoustic wave propagation problem addressed in this program. An ideal infinitesimally short pulse of acoustic energy is generated at time $t_o = -R_o/v$ at a distance R_o within the sample. The wavefront is spherical in shape and propagates to the right with velocity v, and at time $t = 0$ its apex just reaches the surface. As the wavefront continues to propagate, the effect on the surface is an elastic disturbance that begins as a point at $r = 0$ and propagates outward as an annular ring of radius r, much like the circular waves that propagate outward from a pebble dropped into a pond of still water. Now the total distance from the point at which the pulse is generated to the annular ring of surface disturbance is defined as R, where

$$R^2 = r^2 + R_o^2 \tag{1}$$

and

$$R = R_o + vt \quad . \tag{2}$$

Combining Equations 1 and 2 yields

$$r = \sqrt{(R_o + vt)^2 - R_o^2} = \sqrt{vt\ (2R_o + vt)} \quad . \tag{3}$$

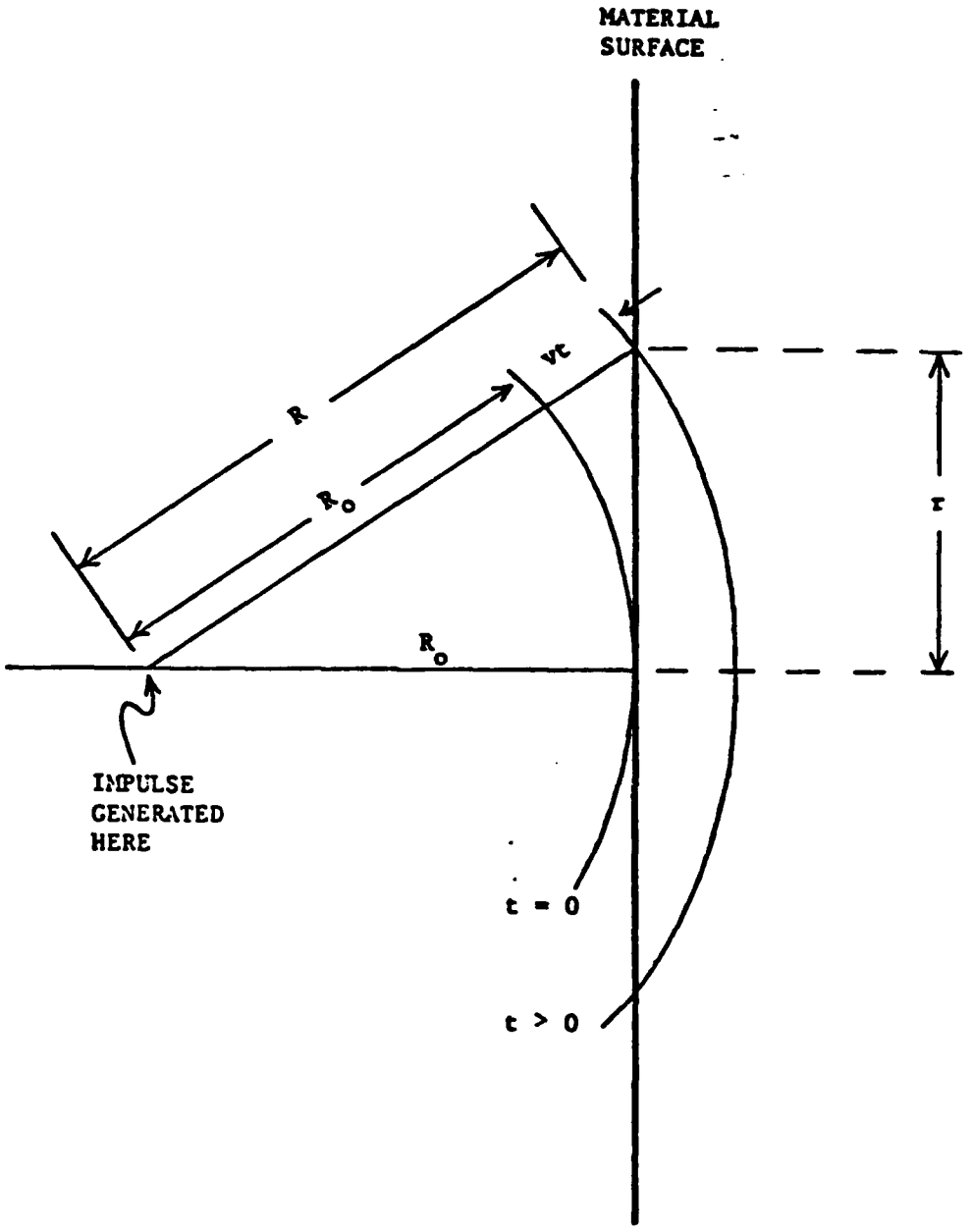

Figure 1. Surface excitation of a focused acoustic impulse.

Equation 3 describes the surface radius (r) of the ring of elastic disturbance as a function of time (t). However, the desire in this program is to generate an impulsive elastic disturbance at the surface that will come to a focus at R_o, and this situation must be reversed. In other words, the disturbance must be an annular ring that shrinks from some maximum radius ($r = r_m$) at $t = 0$ to a point ($r = 0$) at $t = T$. Furthermore, to produce the desired spherical acoustic wavefront, the annular ring must shrink according to the relation

$$r = \sqrt{v(T-t)\ [2R_o + v(T-t)]} \tag{4}$$

where $$T = \frac{\sqrt{R_o^2 + r_m^2} - R_o}{v} \quad . \tag{5}$$

Consider the following example, where

$$\begin{aligned} R_o &= 40 \text{ mm} \\ r_m &= 20 \text{ mm} \\ v &= 6300 \text{ m/sec.} \end{aligned} \tag{6}$$

Substituting this information into Equation 5 yields

$$T = 749 \text{ ns.} \tag{7}$$

If a laser is used to induce a thermoelastic surface disturbance like that described above, it must generate a collimated pulse at least 749 ns long, and a device must be found that will obscure the collimated beam, passing it only through an annular ring that shrinks according to the relationship established in Equations 4 and 5. The electro-optic spatial light modulator (EOSLM) is just such a device.

The basic concept of the EOSLM is illustrated in Figure 2, which is the standard configuration for a longitudinally excited, electro-optic modulator[6] with one exception: one end face of the electro-optic crystal is conic in shape. In a standard electro-optic modulator, where the length of the crystal does not vary with radius, the maximum optical transmission occurs when the product of the applied voltage (V) and the length (L) are equal to a constant that is determined by the electro-optic material and the configuration of the modulator, i.e.,

$$VL = k \quad . \tag{8}$$

However, in the modulator proposed here, the relationship of Equation 8 holds true only for an annular ring about the optic axis. Furthermore, as the applied voltage is reduced, the radius of the annular ring shrinks accordingly, achieving the desired effect.

The Phase I proposal approach was to build and demonstrate programmably focused ultra sound. For reasons discussed later, an alternative device was demonstrated.

2.2 Benefits

If device of the type described is ultimately developed, the result would be a method by which focused ultrasound can be easily scanned in three dimensions within the material under test. The spatial resolution of ultrasonic testing techniques would be radically improved. The ease of the scanning technique and its electronic programmability would result in greater facility for computerized automation and a reduction in the time required to perform a scan. This would eventually allow increased testing with higher sample densities at

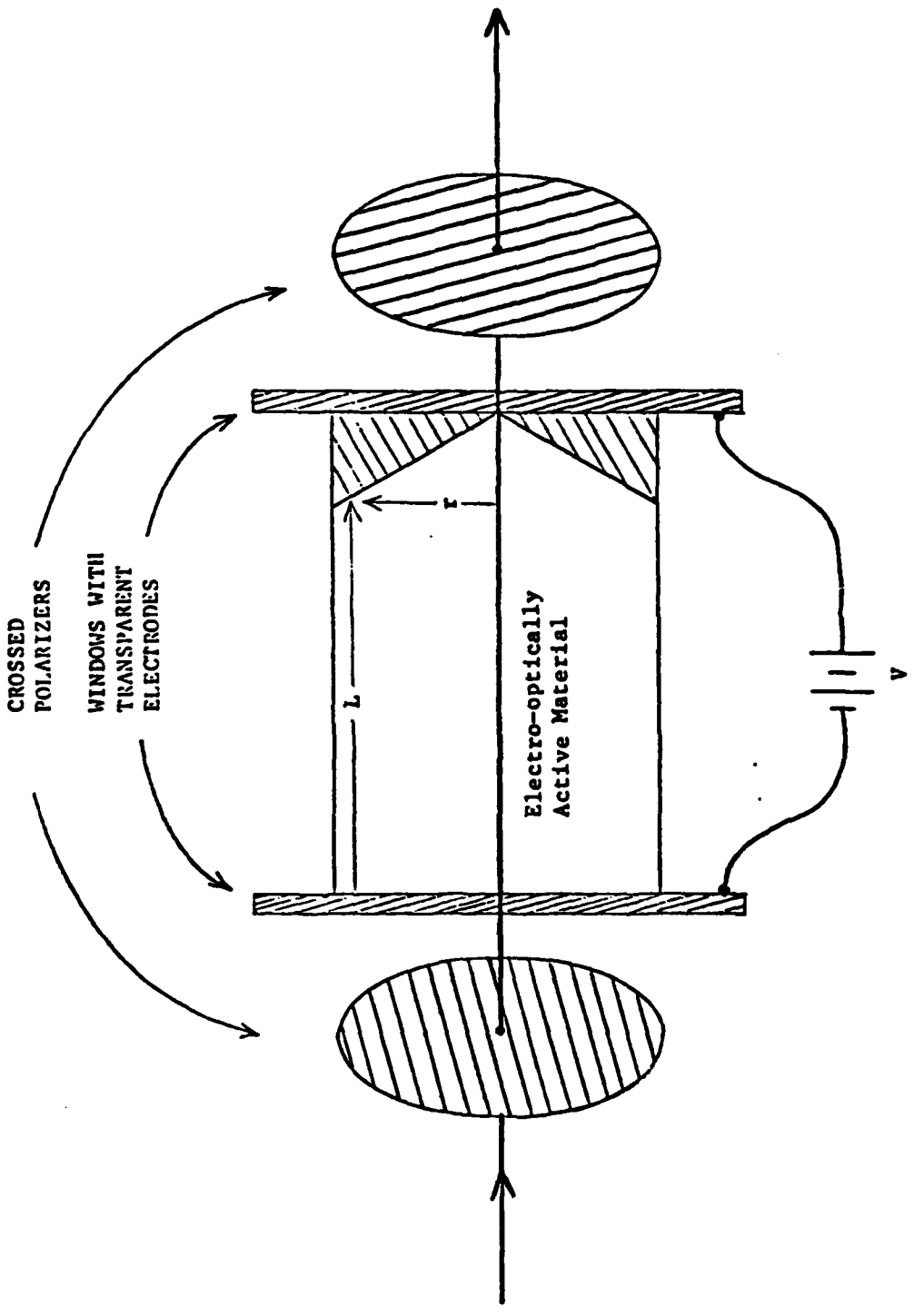

Figure 2. The configuration of the Electro-Optic Spatial Light Modulator (EOSLM).

improved resolution. In many cases the easily scanned, and essentially noncontact nature of the technique would make possible in situ testing to determine if critical components had deteriorated with age or use. The ultimate impact would be greater reliability of critical components and structures, especially in safety critical applications such as aircraft and spacecraft components, high speed ground travel, and advanced weapons and delivery systems.

2.3 Alternative Approach

A much more simple way to achieve the effect of the collapsing ring of light is to excite a Fresnel zone plate with a rapidly, multiple pulsing laser. The outer ring in the plate generates an acoustic pulse at time t_o which adds along the axis to a pulse generated by inner rings at later times $t_o + \Delta t$. This, in effect, provides a collapsing ring which collapses in steps at a rate determined by the laser pulse separation. Because of the difficulty in manufacturing the EOSLM described above within the scope of the project, the concept was demonstrated with this electronically "programmable" Fresnel plate.

3.0 PHASE I - TECHNICAL OBJECTIVES

The overall objective of Phase I is to answer the question of the feasibility of electro-optically generating a rapidly shrinking ring of surface thermoelastic disturbance to produce focused ultrasound. The intent here is to demonstrate the concept experimentally. Note that because of the limited scope of Phase I, theoretical work, beyond that absolutely necessary to properly define the experiments, will be postponed until Phase II.

To accomplish the overall objective of this program, certain intermediate objectives must be attained in the process. Specifically, they are:

1. produce a Fresnel zone plate design for short rapid laser pulses of spacing, 1-5 μs.

2. fabricate the Fresnel zone plate, laser and electronics according to the design produced in 1), and

3. experimentally demonstrate focused ultrasound.

As with any research program, additional objectives were identified as the work progressed and are addressed in later sections. However, SDL is of the opinion that the objectives listed above are those that are sufficient and necessary to attain the primary objective of feasibility.

4.0 TECHNICAL DISCUSSION

4.1 Analytical Preparation

The concept of the Electro-Optic Spatial Light Modulator (EOSLM) is illustrated in Figure 2. This is essentially the configuration for a longitudinally excited, electro-optic modulator[6] with one exception: one end face of the electro-optic crystal is conic in shape so that its longitudinal length L may be described by the equation

$$L = L_o - \alpha r \tag{9}$$

where r is the radial distance from the optic axis: L_o is the longitudinal distance at the optic axis; and α determines the taper angle of the conic end face.

The transmission characteristic of such a device is[6]

$$\frac{I}{I_o} = \sin^2 \left[\frac{\pi}{2} \frac{V}{V_\pi} \left(1 - \alpha \frac{r}{L_o}\right) \right] \tag{10}$$

where V is the applied voltage and V_π is a voltage characteristic of the electro-optic material. If, for instance, α is chosen to be

$$\alpha = \frac{L_o}{2R} \tag{11}$$

where R is the maximum radius of the crystal, then

$$\frac{I}{I_o} = \sin^2 \left[\frac{\pi}{2} \frac{V}{V_\pi} (1 - \frac{r}{2R}) \right] \quad . \qquad (12)$$

The upper and middle plots of Figure 3 illustrate the transmission characteristics of such a device for several values of V between V_π and 6 V_π. Note that if V starts high (6 V_π) and decreases, the radial position of the intensity maxima move inward, which is the basic process desired here. However, for a single device there are multiple maxima in the spatial distribution where only one is desired. To overcome this, or at least improve the situation, two devices can be placed in series and driven simultaneously. The upper and middle plots of Figure 3 were chosen to illustrate this, i.e., if one device is driven with a voltage decreasing from 2 V_π to V_π (upper curve), and the other device is driven simultaneously with a voltage decreasing from 6 V_π to 3 V_π (middle curve), the lower plot of Figure 3 is the combined spatial transmission characteristic that results. Mathematically, the two devices correspond to two components of a Fourier series and it is theoretically possible to produce any desired transmission characteristic by cascading a sufficient number of EOSLM's. But the reduction in the extraneous maxima in the lower curve of Figure 3 appears to be sufficient for the problem at hand, and hence, two devices may be all that are necessary.

A detailed design effort is required, though. Typically V_π is 10,000 volts for an ADP crystal, an especially prohibitive value when considering drive voltages as high as 6 V_π. But this can be radically

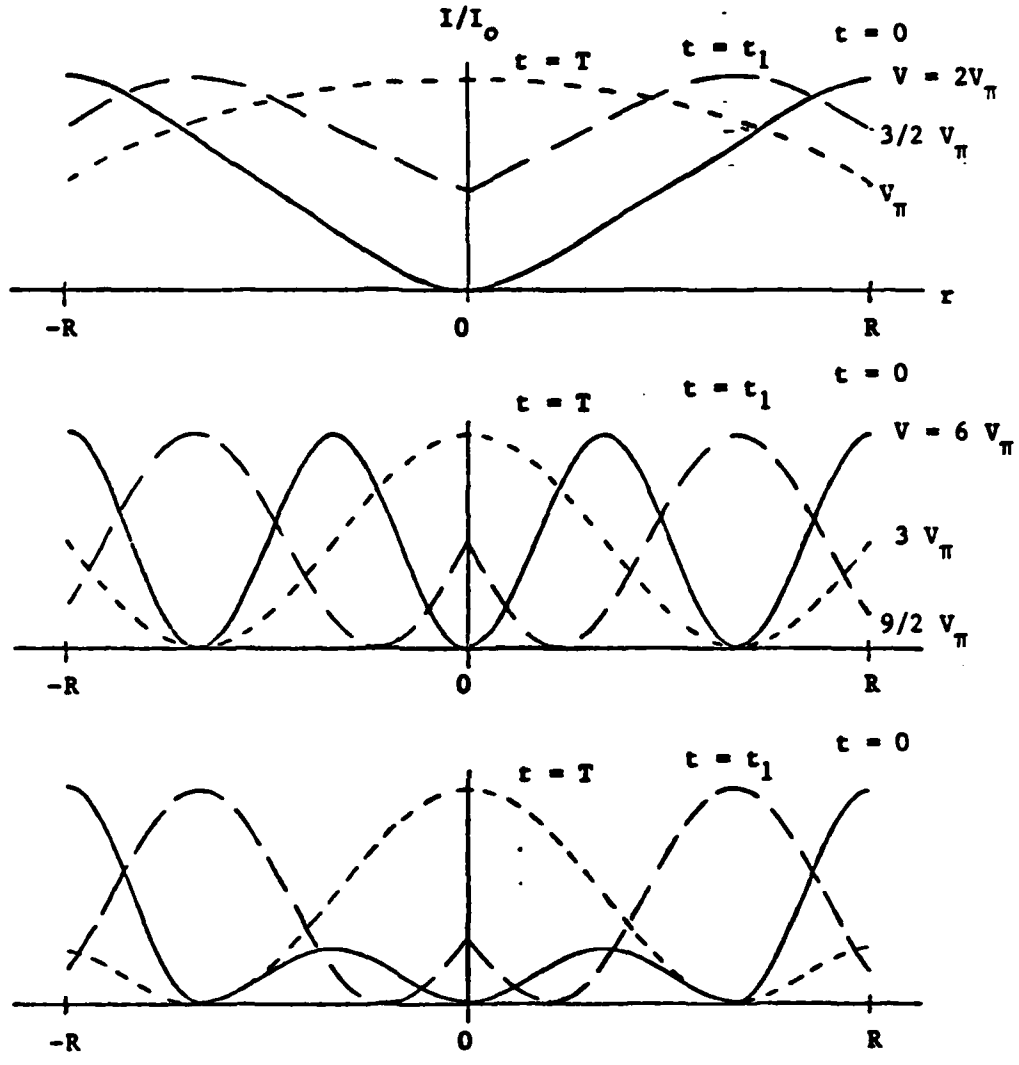

Figure 3. The spatial transmission characteristic of an Electro-Optic Spatial Light Modulator and its variation with drive voltage.

improved by transverse rather than longitudinal excitation of the electro-optic material[7,10]. Furthermore, instead of driving two identical devices with different voltages, it may be possible to drive two different devices (different α) with the same voltage. In any case, the potential exists for programing the drive voltage so that the position of the annular ring corresponds identically to that described by Equation 4. Also note that the drive requirements are not severe. The drive voltage here need only be ramped, rather than stepped, during a period of several hundred nanoseconds, whereas Q-switch drives must commonly step several thousand volts in 10's of nanoseconds.

Task 1 - EOSLM Design

A major task in Phase I was be to determine the proper design of the EOSLM. The various aspects of the design of electro-optic modulators have been studied for many years and are known and well documented[6,10]. However, they are optimized for wide bandwidth operation at low drive voltage with flat, parallel crystal faces. And while low drive voltage is desirable in the EOSLM, its required bandwidth is far lower than that of a typical e-o modulator. This could be used to advantage in the design of the EOSLM.

The basic goal of this task was to produce a design for a transversely excited EOSLM with an acceptably low V_π. In standard modulators the lowest drive voltages are achieved by using 45° X and/or Y cut crystals of ADP or AD*P. They make use of the high value of the r_{41} electro-optic coefficient to reduce V_π. Such crystals are readily available, and estimates have been obtained concerning polishing of the

conic surfaces. Unfortunately, this configuration exhibits increased thermal instability and walkoff due to natural birefringence. Compensation is successfully accomplished by properly orienting four matched crystals in each modulator[10].

Alternately, it may be advantageous to employ transverse excitation of the somewhat lower r_{63} electro-optic coefficient in 45° Z cut ADP or AD*P crystals. It should be possible to achieve a V_π of 600 to 1000 volts, and in this configuration compensation only requires two matched crystals in each modulator. Z cut crystals, however, are not as readily available as the X and Y cuts.

The design will also have to include consideration of refraction effects at the conic surface. It may be possible to compensate by using external passive conic optical components, but the most likely method will be proper choice of the index matching fluid used in the EOSLM. Cargille is a strong candidate here since it provides an excellent index match to ADP and can withstand optical power densities up to 100 MW/cm^2.

Designs were also considered for:

1. a sealed housing for the crystals with transparent antireflection coated windows and high voltage isolation of the parallel plate crystal mounts, and

2. the high voltage drive electronics.

Task 2 - EOSLM Fabrication and Preliminary Testing

After the preliminary design of the EOSLM was completed, we attempted to locate a vendor for the complete component. We were unable to find a vendor who was willing to meet the required specifications within the time and cost constraints of the program. Therefore, we directed the experimental part of the program to demonstrate the concept in an alternate way.

Task 3

Figure 4 illustrates the configuration. The effective collapsing light ring is generated by pulsing a ruby laser against a Fresnel zone plate with pulse separation providing an effective focal length as described in the next section.

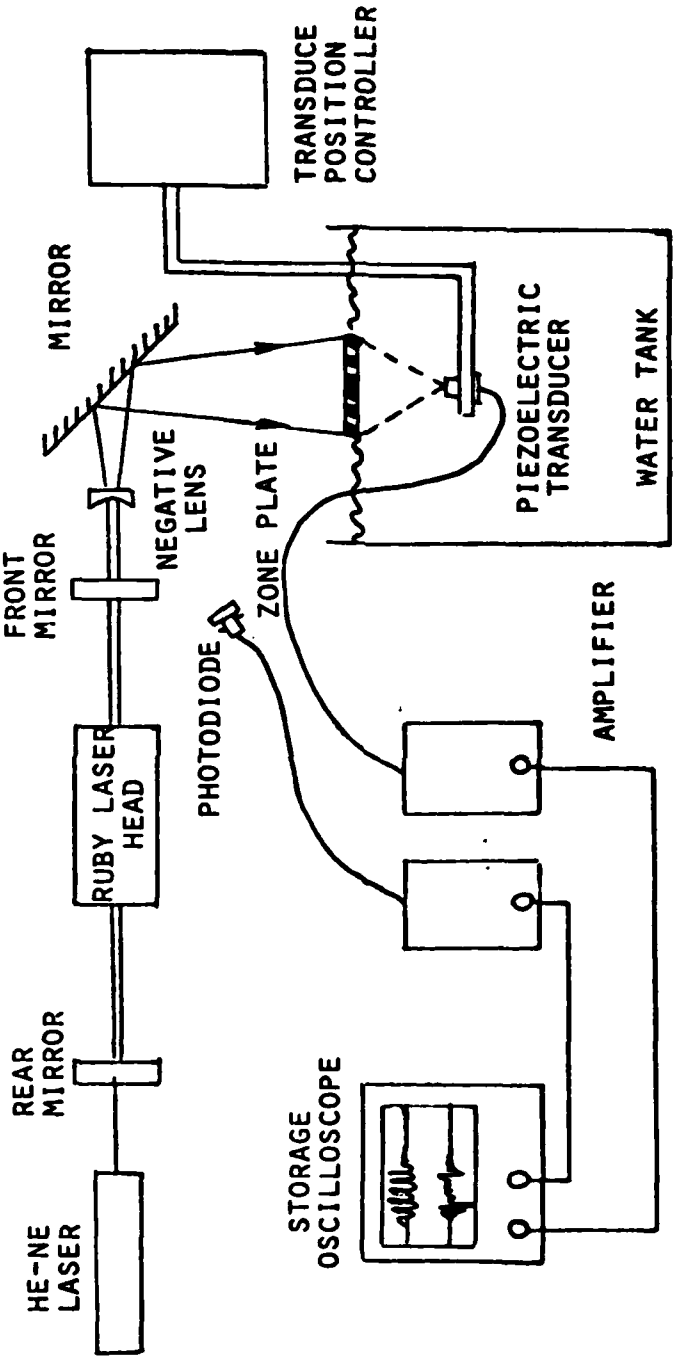

Figure 4. Task 3 experimental apparatus.

5.0 PHASE I - EXPERIMENT

5.1 Experiment Apparatuses

An experiment was designed in which thermoelastically induced focused ultrasound, by using a high power pulsed laser to thermally induce elastic stress in the surface of the Fresnel zone plate, has been investigated in water.

A photograph of the experiment setup is shown in Figure 5. The output beam of the ruby laser is expanded and directed downward into an experimental water tank, in which a Fresnel zone plate is placed on the water surface. Absorption of the laser energy occurs in the discrete black annular zones by a thin epoxy layer that was previously deposited on the lower surface, which contacts with water surface, of the zone plate. A piezoelectric transducer (2.25MHZ, 15" diameter) is used as a receiver to measure the acoustic energy intensity at the desired spots in water. Water is chosen to provide excellent acoustic coupling to the transducer. An amplifier (B & K charge amplifier 2635) is used to magnify the transducer output signals. The transducer can be scanned in three dimensions by using a remote controlled translation stage. A photodector is used to measure the laser radiation intensity, and a storage scope triggered by the laser power supply is used to monitor both the optical and acoustic signals at the same time. The optical system is aligned by using a helium-neon laser.

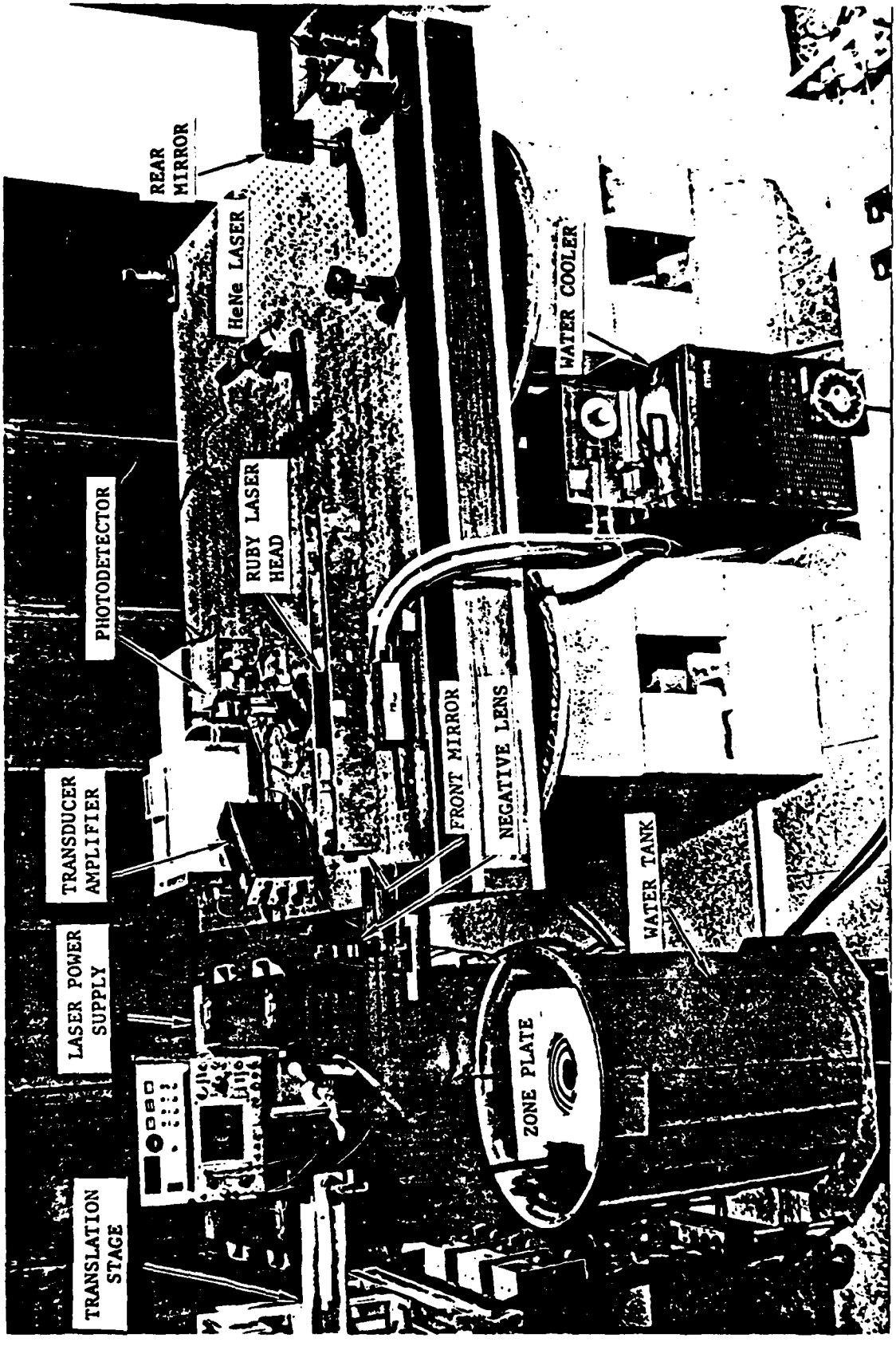

Figure 5. Experimental Setup.

Laser Characteristic

The ruby laser that we used is comprised of a 3-in by 3/8-in ruby rod (0.05% doping), a helical flashlamp and two flat mirrors. The laser radiation patterns showed that the laser pulse separations were randomly distributed and about half of them were around 5msec.

5.2 Fresnel Zone Plate

The Fresnel zone plate is a diffraction grating with focusing properties. The radii of the set of circular fringes with maximum absorption of optical energy is

$$rn = (f\lambda)^{1/2} (\eta)^{1/2} \qquad (13)$$

where

f: focal depth in testing material

λ: accoustic wavelength in test material

η: 1,3,5 .....

The acoustic wavelength in testing material is

$$\lambda = v \times \Delta t \qquad (14)$$

where v is the sound speed within the testing material; and Δt is the laser pulse separation. The frequencies of the ultrasound generated by the thermoelastic conversion process is entirely dependent upon the temporal characteristics of the laser source. According to the

structure of laser output, most of the pulse separations are 5msec which infers that the wave length of the ultrasound in water is 7.4mm. Figure 6 shows that a zone plate can be constructed by drawing on white paper concentric circles whose radii are proportional to the square roots of consecutive integers 1,2,3 .... These form annual zones, every other one of which is to be blackened. This done, the figure is photographically reduced to a desired size, and the resulting transparency is the zone plate.

The first zone plate that we used to generate ultrasound in water was designed to have a lcm focal depth. The ruby laser rod beam was expanded to 3-in diameter, at the time when it hit the zone plate, by passing the beam through a -80mm focal length plano-concave lens. The transducer was scanned in three dimensions. The test conditions are listed in Table I.

5.3 Experiment

Figure 7 shows the energy intensity profile of the thermo-elastically induced ultrasound along the axial axis of the zone plate in water. It depicts that the induced ultrasound energy does focus to a point on the axial axis which has a lcm focal depth, and that agrees with the theoretic designed focal length.

During the time the transduced was scanned in a horizontal plane, along two radial axes, which intersect at a right angle at the focal point, the transducer output signals oscillated up and down and had a lowest reading at the focal point. It was found that most of the peak reading occurred when the transducer took a measurement right under the

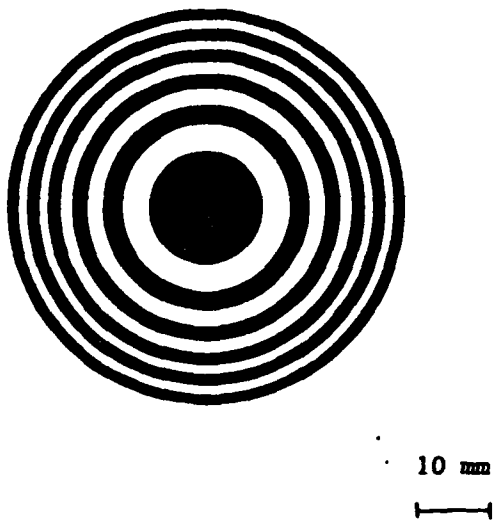

Figure 6. Fresnel Zone Plate.

TABLE I

TEST CONDITIONS FOR ZONE PLATE NO. 1

RUBY LASER (HOLOBEAM 300)			TRANSDUCER		AMPLIFIER	
CAVITY LENGTH (inch)	PUMPING VOLTAGE (V)	AVERAGE PULSE SEP. (μsec)	TRANSDUCER SENSITIVITY DIAL	OUTPUT RATING $(\frac{MV}{unit\ out})$	UPPER FREQ. LIMIT (Hz)	LOWER FREQ. LIMIT (Hz)
22	4000	5.0	8.30	10	>100K	21

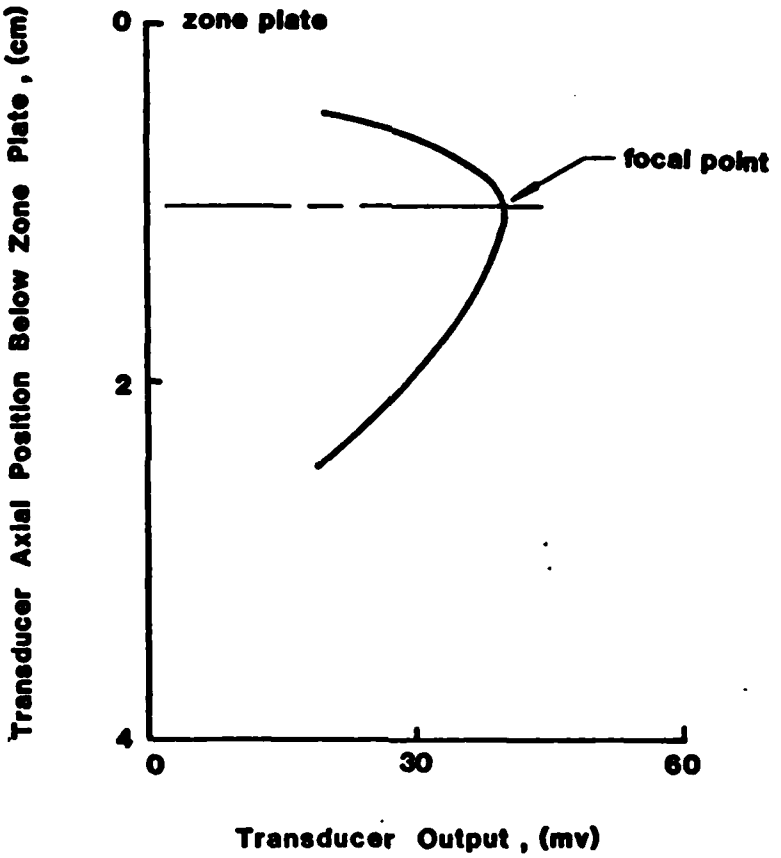

Figure 7. Ultrasound intensity profile on axial axis

transparent zones, at which part the optical energy went through the transparent areas and hit the transducer face. The transducer has a half-inch diameter black sensing face, which will absorb the optical energy if it is directly hit by the laser light.

Laser Modifications

The radiation pattern of the ruby laser with a 22-in separation between the two flat mirrors, showed a varity of high order mode outputs which induced noises on the transducer output signals. In order to minimize the high order mode without sacrificing the laser output energy, the optical resonator was modified by extending the laser cavity length from 22-in to 133-in, and the flashlamp pumping voltage was raised from 4000v to 4300v. After the above changes, the structure of the laser radiation patterns showed that the appearance of the high order modes was reduced and the average pulse separations were increased to 10msec, which infers that the average wavelength of the ultrasound is 14.8mm.

Zone Plate

The second zone plate has the following features: a 10cm focal length which is based on the 14.8mm sound wavelength in water, the transparent areas between black zones are covered by reflective material, mylar film, which has a mirror-like reflecting surface so that no laser light can go through the zone plate.

The laser rod beam was expanded by passing it through a -29mm focal length plano-concave lens and at the time when the light hit the

zone plate the beam diameter was 6 inches. The transducer was scanned in three dimension. Figure 8 shows the zone plate and the positions on the two radial axes, X and Y, at which we took measurements. The test conditions are listed in Table II.

5.4 Results

A sample of the results are presented here; Figures 9a to 9e show the photographs of the laser output structures and the induced ultrasound energy patterns. According to the zone plate, every 3, or more than 3, consecutive laser pulses with equal time separation will generate focusing acoustic waves. The time to be needed by the sound wave to travel between the zone plate and transducer face is determined by the distances between the transducer face and the zone plate, and between the transducer face and the focal point.

The average energy intensity of the ultrasound generated by each laser radiation was measured individually by measuring the relative absorption efficiency of the optical energy through each measuring point. Characteristic intensity distributions of the induced accoustic energy was evaluated at constant optical energy. The test conditions are listed in Table III. The relative absorption efficiency is the transducer output measured relative to one unit photodetector output.

Figures 10a to 10c show the dependence of the acoustic energy distribution on the depth within the test material and the horizontal distance from the focal point. It demonstrates the accuracy of the measurement technique. Figures 10b and 10c show a narrow energy intensity distribution is obtained at the focal point along the two

orthogonal radial axes, which shows that the induced ultrasound was focused in three dimensions.

An important feature of the zone plate; focusing of the thermoelastically induced ultrasound can be accomplished by the Fresnel zone plate and the depth of the focused energy within the test material can be predetermined and programmed by changing the laser pulse frequency.

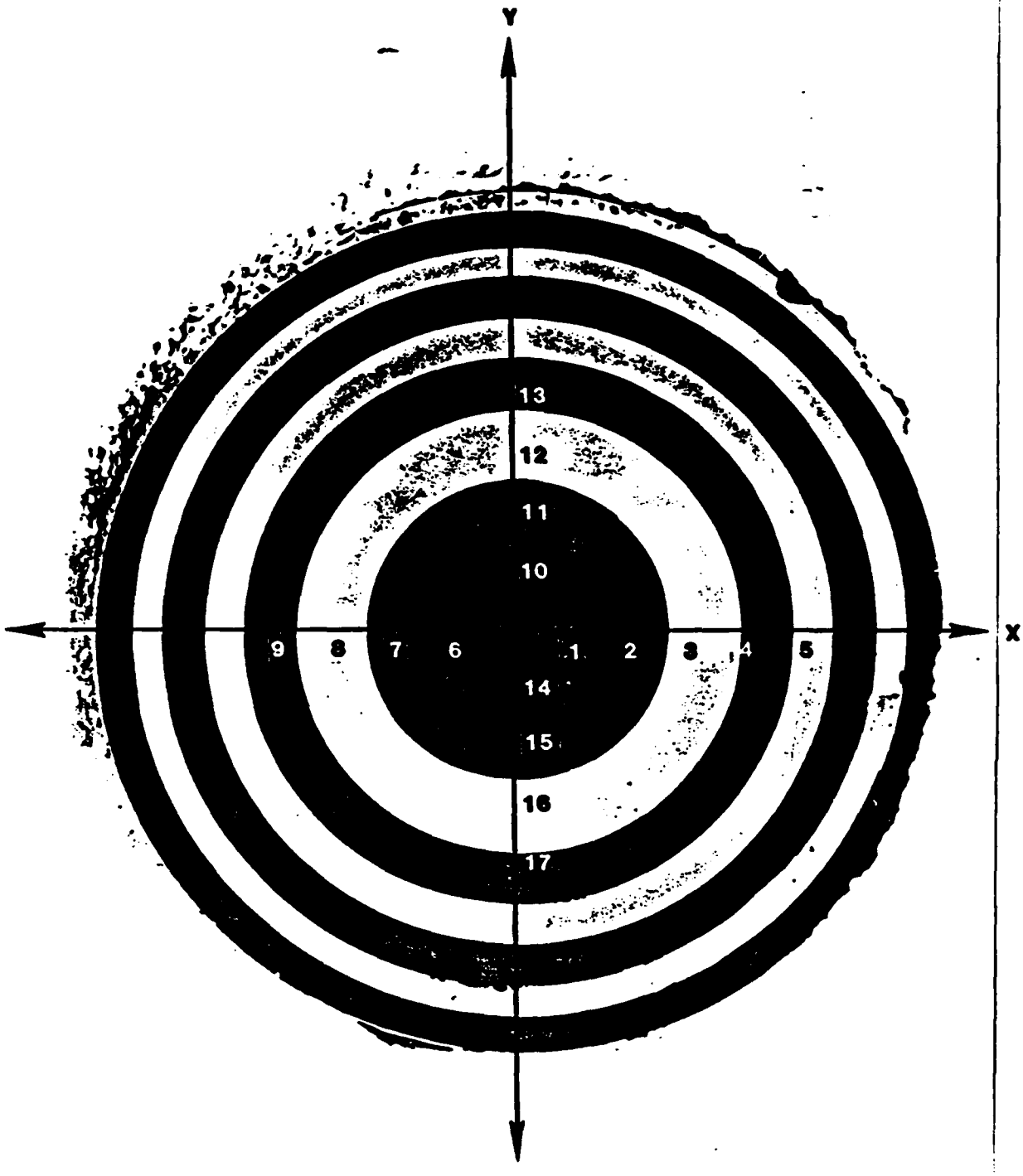

Figure 8. Fresnel Zone Plate.

TABLE II

TEST CONDITIONS FOR ZONE PLATE NO. 2

RUBY LASER (HOLOBEAM 300)			TRANSDUCER		AMPLIFIER (B&K 2635)	
CAVITY LENGTH (inch)	PUMPING VOLTAGE (V)	AVERAGE PULSE SEP. (μsec)	TRANSDUCER SENSITIVITY DIAL	OUTPUT RATING $\left(\frac{\text{MV}}{\text{unit out}}\right)$	UPPER FREQ. LIMIT (Hz)	LOWER FREQ. LIMIT (Hz)
133	4300	10	3.00	100	>100K	2

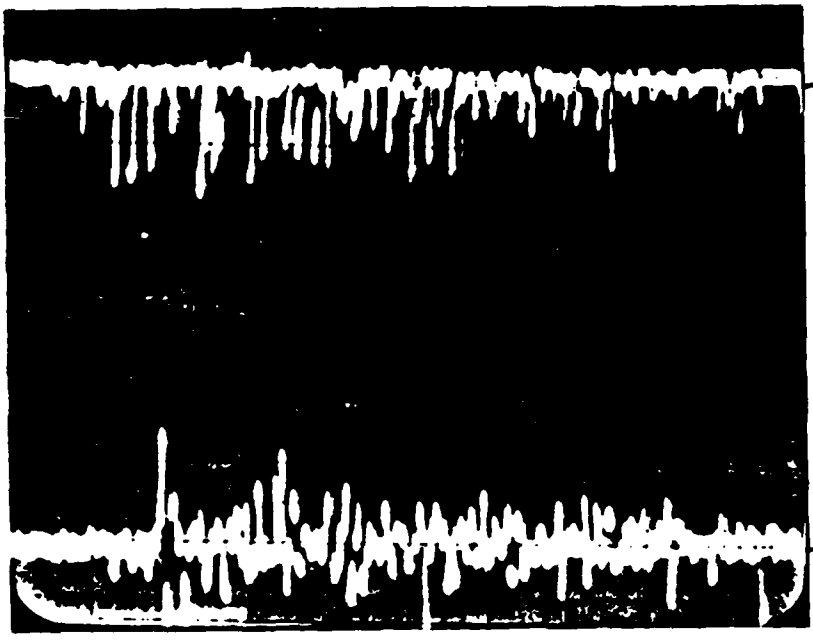

Figure 9a. Structures of the laser output and the induced ultrasound. The transducer was placed at 3 cm under the center of the zone plate.

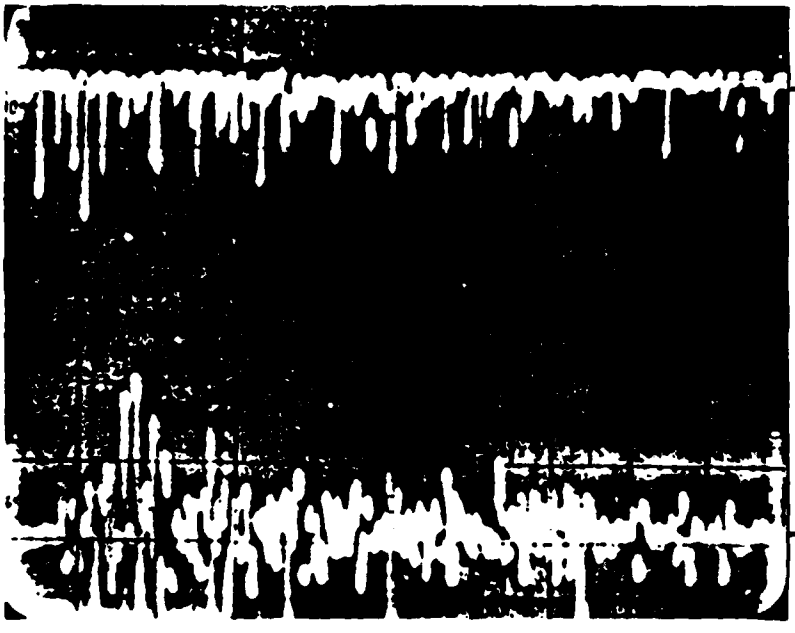

Figure 9b. Structures of the laser output and the induced ultrasound. The transducer was placed at 5 cm under the center of the zone plate.

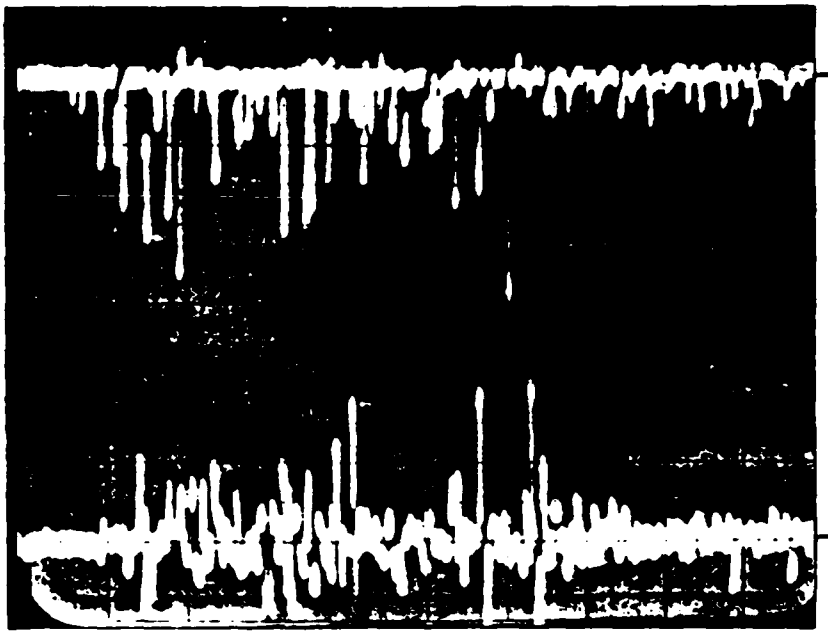

Figure 9c. Structures of the laser output and the induced ultrasound. The transducer was placed at 9 cm under the center of the zone plate.

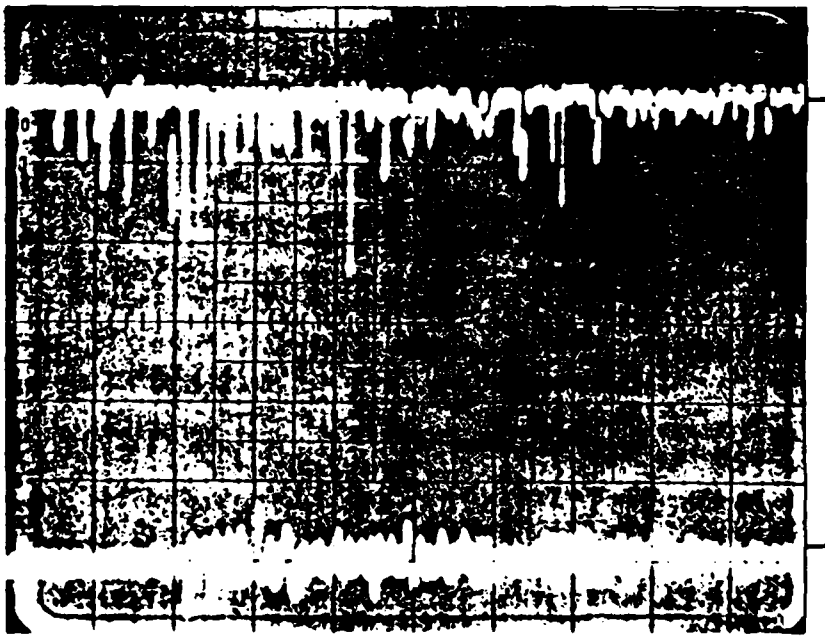

Figure 9d. Structures of the laser output and the induced ultrasound. The transducer was placed at position 13 on the radial Y axis.

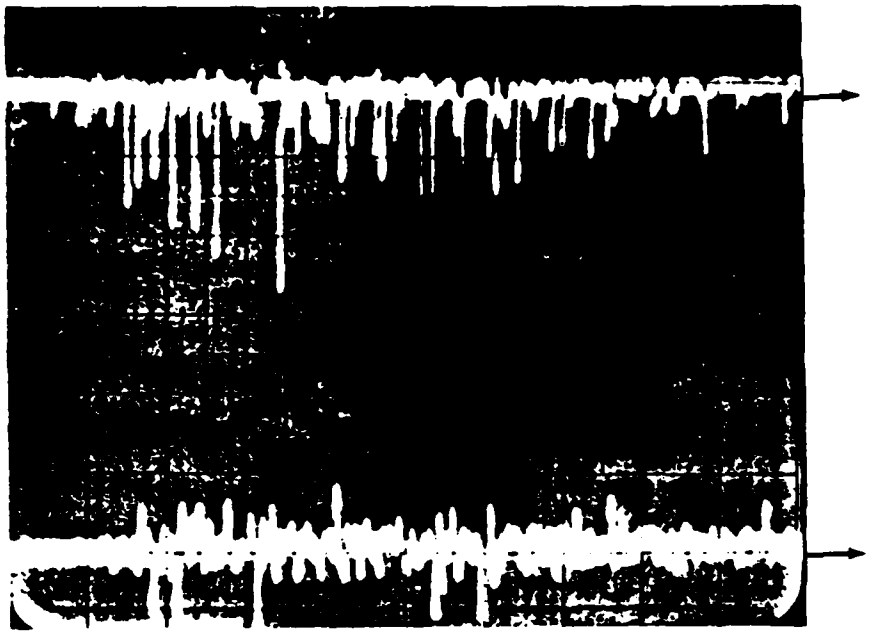

Figure 9e. Structures of the laser output and the induced ultrasound. The transducer is placed at position 16 on the radial Y axis.

TABLE III

TEST MATRIX

TRANSDUCER POSITION	AXIS	PHOTODETECTOR OUTPUT (V)	TIME DELAY (μsec)	TRANSDUCER OUTPUT (MV)	RELATIVE ABSORPTION EFFICIENCY
1	Axial Axis (The position is the distance between the tranaducer and the zone plate)	7.4	7	18.3	2.5×10^{-3}
2		8.0	13	28.7	3.6×10^{-3}
3		6.5	20	26.0	4.0×10^{-3}
4		7.8	26	35.7	4.6×10^{-3}
5		7.5	33	37.5	5.0×10^{-3}
6		8.3	40	40.3	4.8×10^{-3}
7		6.3	46	25.7	4.1×10^{-3}
8		6.5	53	16.0	2.5×10^{-3}
9		8.7	59	13.3	1.5×10^{-3}
1	Radial Axis X (See Figure 8)	7.4	28	20.0	2.7×10^{-3}
2		7.4	23	24.0	3.2×10^{-3}
3		6.5	18	17.7	2.7×10^{-3}
4		7.7	13	8.0	1.0×10^{-3}
5		8.5	8	5.0	0.6×10^{-3}
6		7.8	28	16.7	2.1×10^{-3}
7		7.3	23	9.0	1.2×10^{-3}
8		10.0	18	11.3	1.1×10^{-3}
9		8.0	13	5.0	0.6×10^{-3}
10	Radial Axis Y (See Figure 8)	7.0	28	12.3	1.8×10^{-3}
11		7.7	23	21.6	2.8×10^{-3}
12		8.3	18	14.0	1.7×10^{-3}
13		7.8	13	5.0	0.6×10^{-3}
14		8.6	28	5.0	0.6×10^{-3}
15		8.7	23	7.3	0.8×10^{-3}
16		11.3	18	10.0	0.9×10^{-3}
17		8.2	13	5.0	0.6×10^{-3}

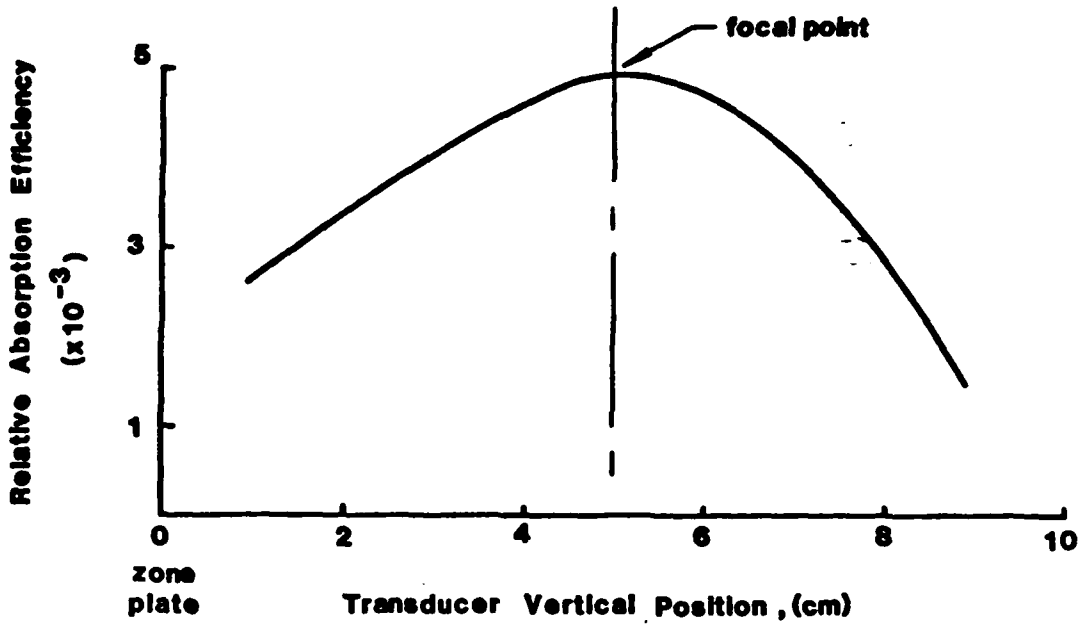

Figure 10a. Ultrasound intensity profile on axial axis.

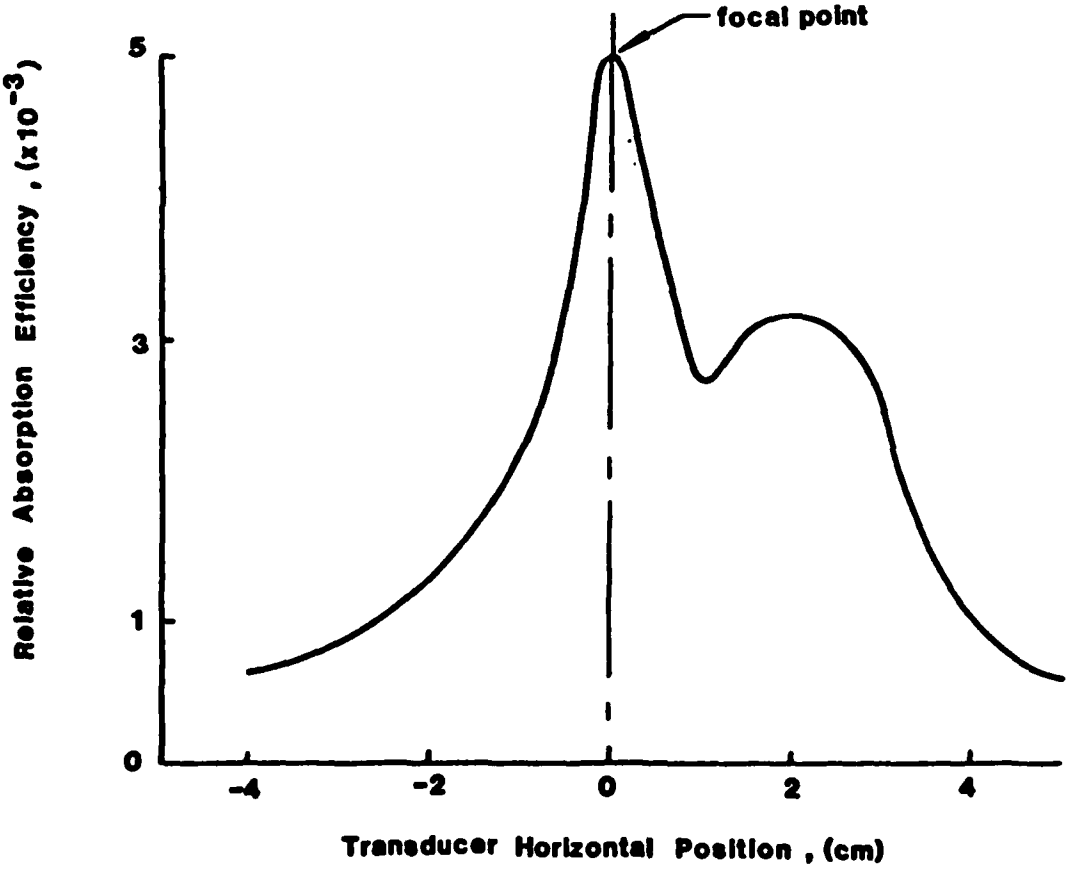

Figure 10b. Ultrasound intensity profile on radial axis X.

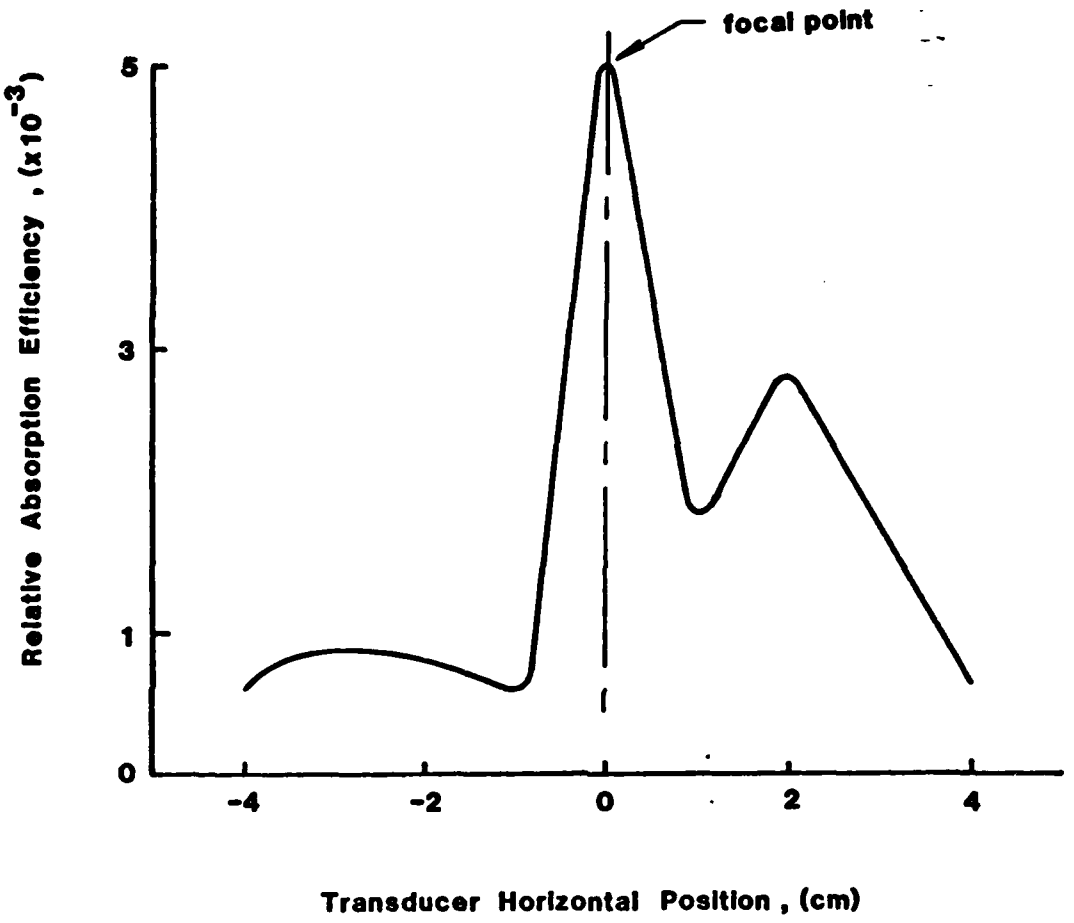

Figure 10c. Ultrasound intensity profile on radial axis Y.

6.0 SUMMARY AND RECOMMENDATIONS

In the foregoing research, we have demonstrated analytically and experimentally that a collapsing ring of light directed onto a target surface will create ultrasound which is focused into the target at a distance dependent upon the rate of collapse. An electro-optic modulator was designed to produce a programmable collapsing ring of light. After the completion of the preliminary design, it was determined that, while possible to construct such a system, no vendor could produce the system with guaranteed specifications and within the time and cost constraints of the program.

Therefore, the collapsing ring concept was demonstrated by illuminating a properly designed zone plate with pulsing laser radiation. This emulated a ring of light which collapses in a stepwise fashion. The system was shown to focus as expected to a distance which is directly proportional to the pulse separation. Although this method demonstrates the validity of the concept, it is not itself a viable way to achieve a collapsing ring in practice.

Therefore, before Phase II research could be justified, suitable hardware is required to perform this function. Our experience to date has not provided us with a source of the required hardware. Therefore, we do not recommend Phase II research until such a device can be built, whether it be the variety designed herein or of some other variety.

7.0 REFERENCES

1. Krautkrämer, Josef and Krautkrämer, Herbert, Ultrasonic Testing of Materials, Springer-Verlag, New York, N.Y., (1977).

2. Thompson, R. B., "Electromagnetic Generation of Ultrasound", Proceedings of a Workshop on Nondestructive Evaluation of Residual Stress, NTIAC-76-2, pp. 219-226, San Antonio, Tx., August 13-14, 1975.

3. White, R. M., IRE Trans. Instr. I-II, 294 (1962).

4. White, R. M., J. Appl. Phys. 34-12, 3559, (1963).

5. Stone, John M., Radiation and Optics: An Introduction to the Classical Theory, McGraw-Hill, Inc., New York (1963).

6. Yariv, Amnon, Introduction to Optical Electronics,. Holt, Rinehart and Winston, Inc., New York (1971).

7. J. M. Ley, Electronics Letters, 2, 12 (1966).

8. B. Trevelyan, J. Phys. E, 2, 425 (1969).

9. K. Hookabe and Y. Matsuo, Electronics Letters, 6, 550 (1970).

10. G. E. Francois and F. M. Librecht, Appl. Opt., 11, 472 (1972).

11. von Gutfeld, R. D., Ultrasonics, 175, July (1980).

12. Hutchins, D. A., Dewhurst, R. J., and Palmer, S. B., Ultrasonics, 103, May (1981).

13. Wikramasinghe, H. K., Bray, R. C., Jipson, V., Quate, C. F., and Salcedo, J. R., Appl. Phys. Lett. 33, 923, (1978).

END

FILMED

4-85

DTIC